Heavy Ion Radiation Assessment of a 100G/200G Commercial Optical Coherent DSP ASIC

Raichelle Aniceto*[a,b], Randall Milanowski[c], Steve McClure[c], Alexa Aguilar[a,b], Slaven Moro[a], Eric D. Miller[a], Kerri Cahoy[b]

[a]Facebook Connectivity Lab, 8500 Balboa Blvd. Northridge, CA 91239; [b]Massachusetts Institute of Technology, 77 Massachusetts Ave., Cambridge, MA 02139; [c]M&A, Inc., 2726 Shelter Island Drive #268, San Diego, CA 92106;

ABSTRACT

We assess the viability of a state-of-the-art 100G/200G commercial optical coherent DSP ASIC (16 nm FinFET CMOS technology) for space applications through heavy ion testing to (1) screen for destructive SELs and (2) observe for non-destructive heavy ion SEEs on the ASIC. The ASIC was exposed to heavy ion radiation while operating both optically noise-loaded uplink and downlink to an optical "ground" modem. There were no destructive SEEs observed from the heavy ion radiation test campaign.

Keywords: Optical coherent communication; space radiation effects; commercial optical transceiver; DSP ASIC

1. INTRODUCTION

Technological advancements, particularly optical coherent DSP ASICs and photonic integrated circuits (PICs), from terrestrial communications industry have enabled high capacity optical coherent communication systems of 100 Gbps and greater. The standardization of coherent commercial off the shelf (COTS) components through Optical Internetworking Forum (OIF) implementation agreements (IAs) has created a market for low cost and low lead time components with guaranteed performance. There has been recent interest in utilizing optical coherent COTS transceivers for high throughput space applications [1]. Currently, there are no publicly or commercially offered space-grade coherent components that can achieve the data rate performance and meet the cost points of existing telecommunications industry coherent COTS components. To develop optical communications systems for space applications using optical coherent COTS, the performance of commercial optical coherent digital signal processing (DSP) application specific integrated circuits (ASICs) must be evaluated with consideration of space radiation effects.

The space radiation environment has the potential to damage or degrade optical transceiver systems. Proton-induced single event effects (SEEs) in optoelectronic receivers can contribute to link bit error rate (BER), and displacement damage can occur in optoelectronics [2]. Total ionizing dose (TID) effects and SEEs can also damage supporting microelectronics. Our previous work focused on TID and proton SEE assessments of 100G/200G commercial optical coherent ASICs with 28 nm bulk complementary metal oxide semiconductor (CMOS) technology, specifically the Inphi CL20010A1 and Acacia AC100M coherent DSP ASIC [3], [4]. Our previous work has shown the potential of using this technology for a space-based optical coherent communication system. We have observed that commercial optical coherent DSP ASICs are susceptible to proton-induced SEEs, which can lead to system outages. To use commercial optical coherent DSP ASICs, we must characterize SEE-induced ASIC behavior and calculate the SEE rate for the space mission.

This work investigates a 100G/200G commercial optical coherent DSP ASIC manufactured in a 16 nm Fin Field Effect Transistor (FinFET) CMOS technology. There have been observations of increased single event latchup (SEL) sensitivity in FinFET CMOS technologies in comparison to planar CMOS technologies [5]. We assess the viability of state-of-the-art commercial optical coherent DSP ASICs for space applications through heavy ion testing at NASA Space Radiation Laboratory (NSRL) to (1) screen for destructive SELs and (2) observe for non-destructive heavy ion SEEs.

2. EXPERIMENTAL APPROACH

2.1 Test Hardware – 100G/200G Optical coherent Modem with Commercial Coherent DSP ASIC

We developed a 100G/200G optical coherent modem assembly (OMA) to perform radiation testing of the commercial optical coherent DSP ASIC as the device under test (DUT). The optical modem was designed with a commercial CFP2-ACO module as the line-side interface to the ASIC and a 4×28 Gbps QSFP loopback module for the host-side interface. For 200G mode, a 4×28 Gbps CAUI-4 loopback cable served as the second host-side interface. The heavy ion test campaign was performed with the optical modem in 100G mode. The CFP2 module slot was designed with a heat sink and fan. A control loop was implemented, using the fan speed and temperature sensors in the DUT for thermal stabilization of the DUT at the maximum rated junction temperature. ASIC performance data, including the line-side and host-side post-FEC uncorrected errors and pre-FEC BER, as well as ASIC telemetry, including all voltage rails, current rails, and temperature sensors, were collected during tests. Figure 1 shows the 100G/200G OMA developed for radiation testing of the commercial coherent DSP ASIC.

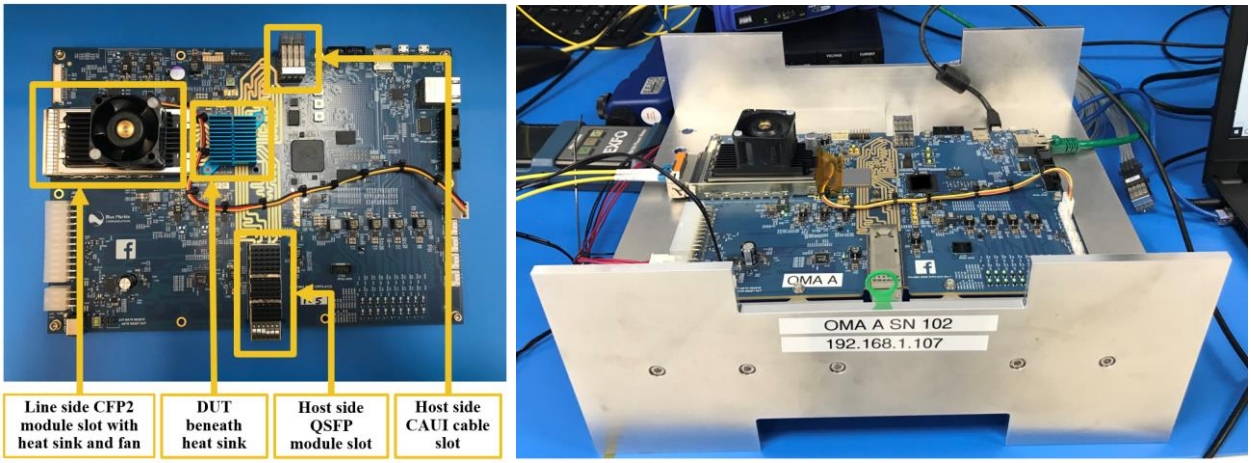

Figure 1. 100G/200G Optical coherent Modem Assembly (OMA) developed for radiation test campaigns of commercial coherent DSP ASIC

2.2 Test Configuration – Noise-Loaded Optical Loopback

Laboratory benchtop testing and heavy ion radiation testing were performed in a noise-loaded optical loopback test configuration between two identical OMAs, one system serving as the test OMA and the other serving as the "ground" OMA (GOMA). Figure 2 shows the laboratory benchtop test setup with GOMA and OMA in noise-loaded optical loopback test configuration.

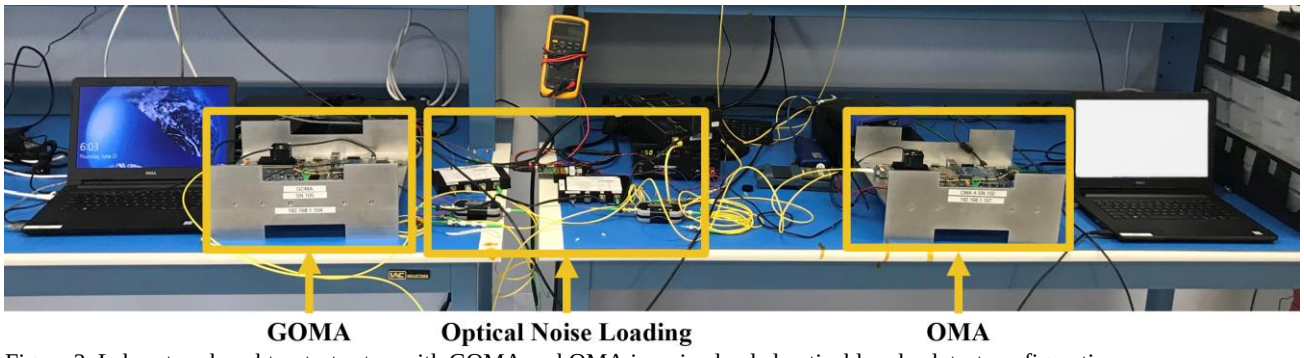

Figure 2. Laboratory benchtop test setup with GOMA and OMA in noise-loaded optical loopback test configuration

The transmit path was noise-loaded to set the optical signal-to-noise ratio (OSNR) level near the ASIC receiver FEC correction threshold. This configuration represents the most stress for the OMA system because the optical communication link is signal-starved and the receiver is operating near the FEC threshold. The noise loading was accomplished by connecting the CFP2-ACO module transmit output to a variable optical attenuator (VOA), which

introduced noise in the system. The VOA attenuation was set 2 dB from the ASIC OSNR threshold. The output of the VOA was input to an erbium doped fiber amplifier (EDFA), which amplified the signal with the introduced noise. The amplifier output was filtered with a 100 GHz optical band-pass filter. Figure 3 shows a block diagram of the noise-load optical loopback test configuration. In addition to the environmental stress induced by optical noise-loading, the ASIC was operated at the maximum rated junction temperature to simulate the worst-case thermal state during testing.

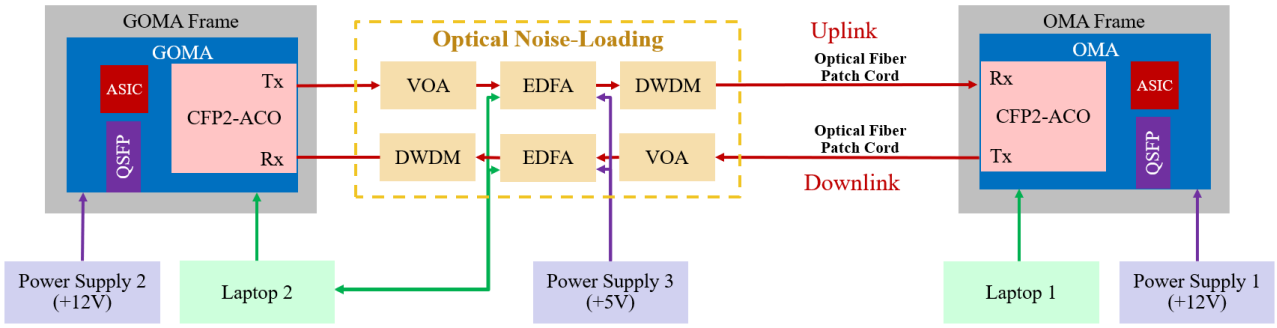

Figure 3. Block diagram of noise-loaded optical loopback test configuration.

2.3 Heavy Ion Radiation Test Campaign

Heavy ion radiation testing was conducted at NASA Space Radiation Laboratory (NSRL) at Brookhaven National Laboratory (BNL) in Long Island, NY. The OMA was fixed to a test stand in-line of heavy ion beam penetration, and a laser was used to align the DUT to the center of the heavy ion beam. Lead blocks were placed in front of the OMA with a small square hole above the DUT area to block the peripheral OMA components from heavy ion radiation and to ensure heavy ion radiation was isolated to the DUT. The test setup equipment for optical noise-loading, GOMA, laptops, and power supplies were set-up on a cart next to the OMA and out of the direct path of the heavy ion beam. Figure 4 shows the heavy ion radiation test setup at NSRL. Figure 4(b) shows the OMA with laser alignment of DUT in the center of the heavy ion beam path and Figure 4(c) shows the lead blocks used to shield the rest of the OMA from heavy ion radiation.

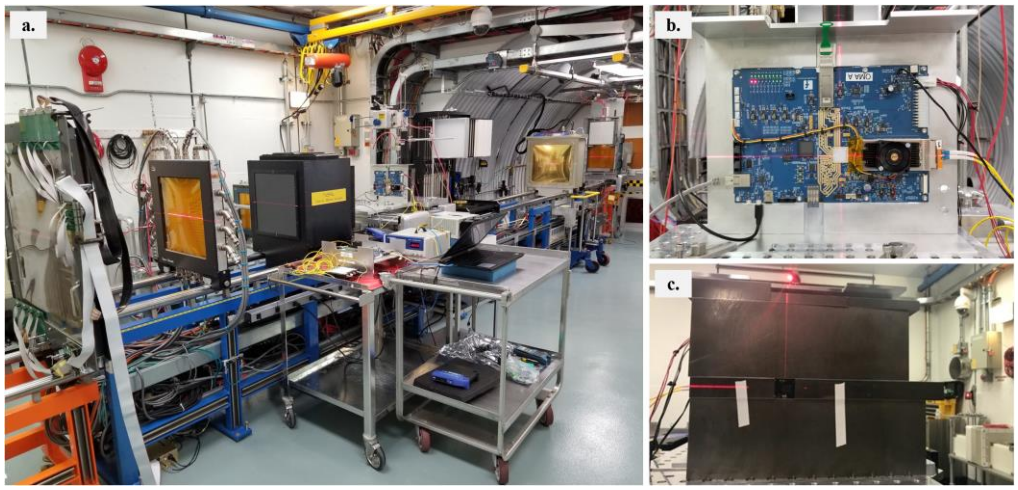

Figure 4. Heavy ion radiation test setup at NSRL. (a) The OMA fixed to a test stand in line of heavy ion beam and (b) the DUT aligned to center of the heavy ion beam path using lasers. (c). Lead blocks used to shield the rest of the OMA from heavy ion radiation.

A pre-radiation test round was completed in the NSRL heavy ion radiation chamber to record baseline data. Figure 5 shows the pre-radiation data set with line and host Post-FEC uncorrected error counts of zero, current values for each voltage rail within nominal range, and stabilized temperature. During the pre-radiation test, no error messages appeared on the DUT GUI console. Since the host-side of the OMA was not noise-loaded or attenuated, the host pre-FEC BER was very low and recorded as a value of 0. Voltage rails V1 and V2 are the digital core voltage power supply. Voltage rails V3 and V4 are the analog power supplies. Voltage rail V5 is the CMOS high speed I/O power supply.

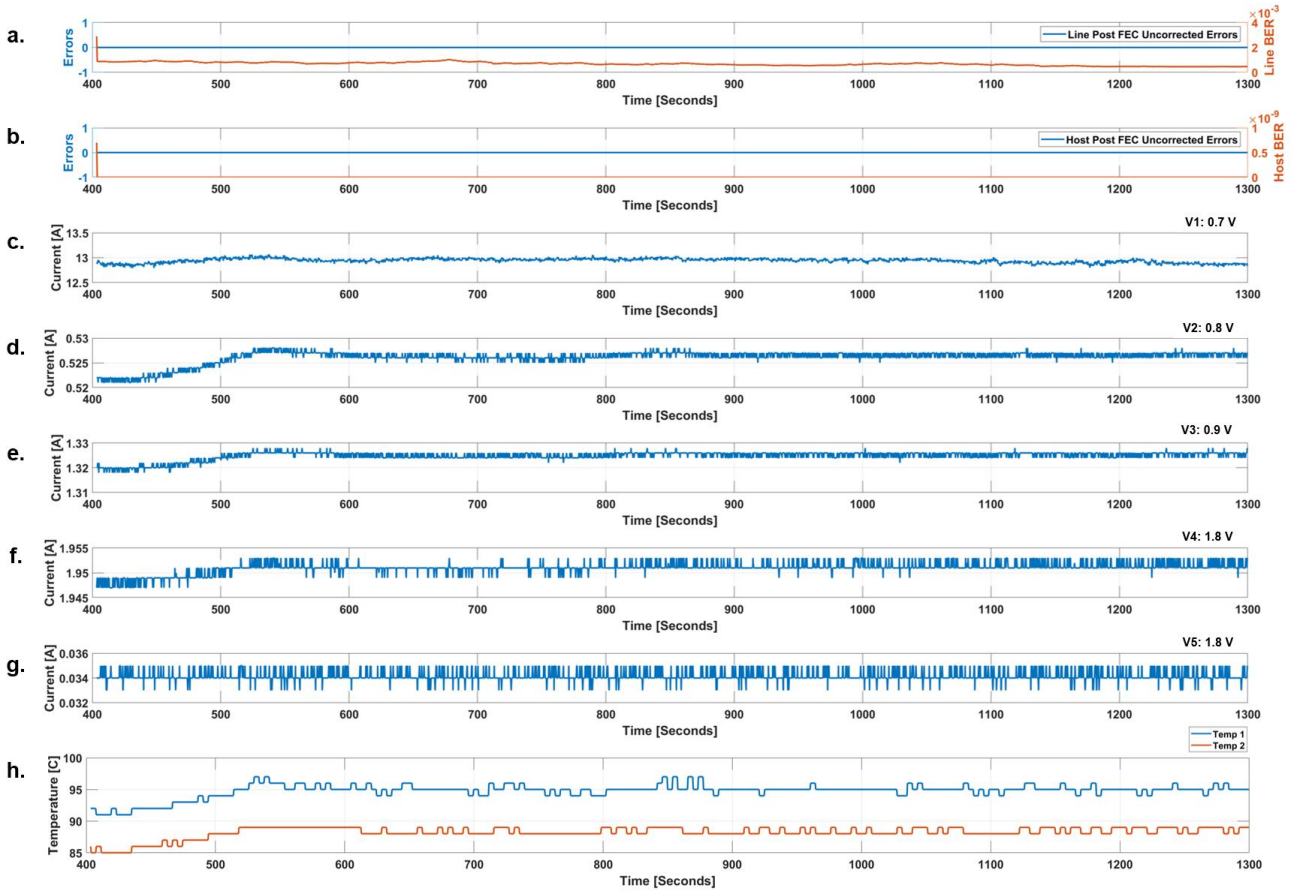

Figure 5. Commercial coherent DSP ASIC pre-radiation data set over ~15 minute time duration. (a) Line post FEC uncorrected errors (left y-axis) and line pre-FEC BER (right y-axis) over time. (b) Host post FEC uncorrected errors (left y-axis) and host pre-FEC BER (right y-axis) over time. (c) Current for voltage rail V1 at 0.7 V. (d) Current for voltage rail V2 at 0.8 V. (e) Current for voltage rail V3 at 0.9 V. (f) Current for voltage rail V4 at 1.8 V. (g) Current for voltage rail V5 at 1.8 V. (h) Temperature sensors of DUT.

The test campaign consisted of ten total irradiation rounds with one radiation round of 3.6 GeV Carbon ions and nine radiation rounds of 46.2 GeV Xenon ions. Each radiation test round generated a different heavy ion linear energy transfer (LET) level. Layers of polyethylene material ranging from 15 mm to 22 mm in 1 mm increments were used to degrade the Xenon ions energy levels to generate higher LET levels of ions penetrating the active region of the DUT. Ions with greater energy level lose energy at a slower rate through material than ion with lower energy level.

The NSRL cyclotron delivers heavy ions in "spills," as a non-uniform flux over time. Each ion spill has a duration of 500 milliseconds over a period of 3.6 seconds. For each radiation test round, the start time of the first ion spill, the radiation end time, and the total irradiation time duration were recorded. The time stamp of observed SEEs and error messages from the DUT GUI console were recorded during each radiation test round. Two types of resets, a soft reset and a hard reset, were used between radiation sets if anomalous behavior persisted or GUI error messages continuously appeared after the end of irradiation. A soft reset included re-running the GUI software to initialize and power sequence the DUT as well as starting a new data file for recorded telemetry. A hard reset included power cycling the OMA then re-running the GUI software.

For the first radiation test round, the DUT was irradiated with 3.6 GeV Carbon ions to a total fluence level of 9.7×10^6 ions/cm^2 over seven sets of irradiation with a total irradiation time of ~ 75 minutes. The first Carbon radiation set had a spill fluence of 200 ions per spill, and the spill fluence was increased for each radiation set up to 20,000 ions per spill. After the Carbon ions test round, we conducted a soft reset of the OMA and GOMA. No SEEs were observed.

For the second radiation test round, the DUT was irradiated with 46.2 GeV Xenon ions to a total fluence of 1.97×10^5 ions/cm^2 over nine radiation sets with a total irradiation time of ~ 86.5 minutes. A spill fluence of 300 ions per spill was

used for the first seven radiation sets. After observing a persistent SEE with continuous GUI error messages in the seventh irradiation set, the spill fluence was decreased to 30 ions per spill for the eighth radiation set. The spill fluence was increased to 100 ions per spill for the last Xenon radiation set.

Due to time constraints at the radiation test facility, we completed each of the eight radiation test rounds with 46.2 GeV Xenon ions and polyethylene degrader in two to five minute time durations. Each radiation round with Xenon ions and polyethylene degrader had a spill fluence of 200 ions per spill and a total fluence ranging from 4602 to 16391 ions/cm^2. A hard reset was performed after each radiation round, with exception to the round #3 with 15 mm polyethylene degrader, to establish separation between data sets of each radiation round. Radiation round #6 with 18 mm polyethylene degrader and radiation round #9 with 21 mm degrader did not require a hard reset since no continuous behavior or GUI error message appeared after the end of the radiation round.

Table 1. Summary of heavy ion radiation test rounds including spill fluence, irradiation time, total fluence, number of SEEs observed, and indication of reset after radiation round.

Round	Ion	Radiation Set	Spill Fluence [ions/spill]	Time [seconds]	Fluence [ions/cm^2]	SEEs Observed	Reset Post Radiation?
1	Carbon	-	200-20000	4500	9.7×10^6	0	Soft Reset
2.1	Xenon	No Degrader – 1	300	1009	15712	2	None
2.2	Xenon	No Degrader – 2	300	227	20003	7	None
2.3	Xenon	No Degrader – 3	300	563	49998	16	None
2.4	Xenon	No Degrader – 4	300	271	22584	4	Soft Reset
2.5	Xenon	No Degrader – 5	300	68	5667	1	Soft Reset
2.6	Xenon	No Degrader – 6	300	327	27250	7	Soft Reset
2.7	Xenon	No Degrader – 7	300	198	16500	7	Soft Reset 2x, Hard Reset
2.8	Xenon	No Degrader – 8	30	1270	8948	1	None
2.9	Xenon	No Degrader – 9	100	1257	30009	11	Hard Reset
3	Xenon	Degrader – 15 mm	200	137	4602	5	None
4	Xenon	Degrader – 16 mm	200	126	6635	5	Hard Reset
5	Xenon	Degrader – 17 mm	200	166	8657	7	Soft Reset, Hard Reset
6	Xenon	Degrader – 18 mm	200	126	6841	4	Hard Reset*
7.1	Xenon	Degrader – 19 mm	200	126	6834	1	Hard Reset
7.2	Xenon	Degrader – 19 mm	200	75	4297	3	Hard Reset
8	Xenon	Degrader – 20 mm	200	173	6834	5	Hard Reset
9.1	Xenon	Degrader – 21 mm	200	126	6472	0	Hard Reset*
9.2	Xenon	Degrader – 21 mm	200	306	16067	4	Hard Reset*
10	Xenon	Degrader – 22 mm	200	306	16391	0	-

3. EXPERIMENTAL RESULTS

We observed a total of 91 non-destructive heavy ion SEEs over all nine radiation rounds. No destructive SEEs were observed. After analyzing the collected data, we categorized the observed SEEs into two main categories: single event upsets (SEUs) and single event functional interrupts (SEFIs). We further categorized similar SEUs and SEFIs into three sub-categories. Table 2 shows a summary matrix for the SEE count of all radiation rounds.

Table 2. Summary matrix of heavy ion single event effects for all radiation test rounds, categorized based on type of single event upset and single event functional interrupt.

Round	Ion	Radiation Set	SEUs				SEFIs				Total SEEs
			A	B	C	Total	A	B	C	Total	
1	Carbon	-	0	0	0	0	0	0	0	0	0
2.1	Xenon	No Degrader – 1	2	0	0	2	0	0	0	0	2
2.2	Xenon	No Degrader – 2	4	2	1	7	0	0	0	0	7
2.3	Xenon	No Degrader – 3	7	8	1	16	0	0	0	0	16
2.4	Xenon	No Degrader – 4	1	1	2	4	0	0	0	0	4

2.5	Xenon	No Degrader – 5	0	0	0	0	1	0	0	1	1
2.6	Xenon	No Degrader – 6	4	0	2	6	1	0	0	1	7
2.7	Xenon	No Degrader – 7	3	2	1	6	0	1	0	1	7
2.8	Xenon	No Degrader – 8	0	1	0	1	0	0	1	1	2
2.9	Xenon	No Degrader – 9	5	4	2	11	0	0	0	0	11
3	Xenon	Degrader – 15 mm	0	4	1	5	0	0	0	0	5
4	Xenon	Degrader – 16 mm	0	3	1	5	0	0	1	1	6
5	Xenon	Degrader – 17 mm	0	6	0	6	0	1	0	1	7
6	Xenon	Degrader – 18 mm	0	4	0	4	0	0	0	0	4
7.1	Xenon	Degrader – 19 mm	0	0	0	0	0	0	1	1	1
7.2	Xenon	Degrader – 19 mm	0	0	1	1	0	1	0	1	2
8	Xenon	Degrader – 20 mm	0	4	1	5	0	0	0	0	5
9.1	Xenon	Degrader – 21 mm	0	0	0	0	0	0	0	0	0
9.2	Xenon	Degrader – 21 mm	0	4	0	4	0	0	0	0	4
10	Xenon	Degrader – 22 mm	0	0	0	0	0	0	0	0	0
Radiation Rounds Total			26	43	13	83	2	3	3	8	91

3.1 Observed Heavy Ion Single Event Upsets

We define a heavy ion induced SEUs as an anomalous event that did not require a soft or hard reset of the OMA to re-establish nominal functionality. After a period of less than 12 seconds, the anomalous behavior disappeared. There were three types of SEUs observed during radiation testing. Figure 6 is a data set from radiation round 2.4 with Xenon ions, showing a total of four SEUs during radiation with labeled according to SEU type.

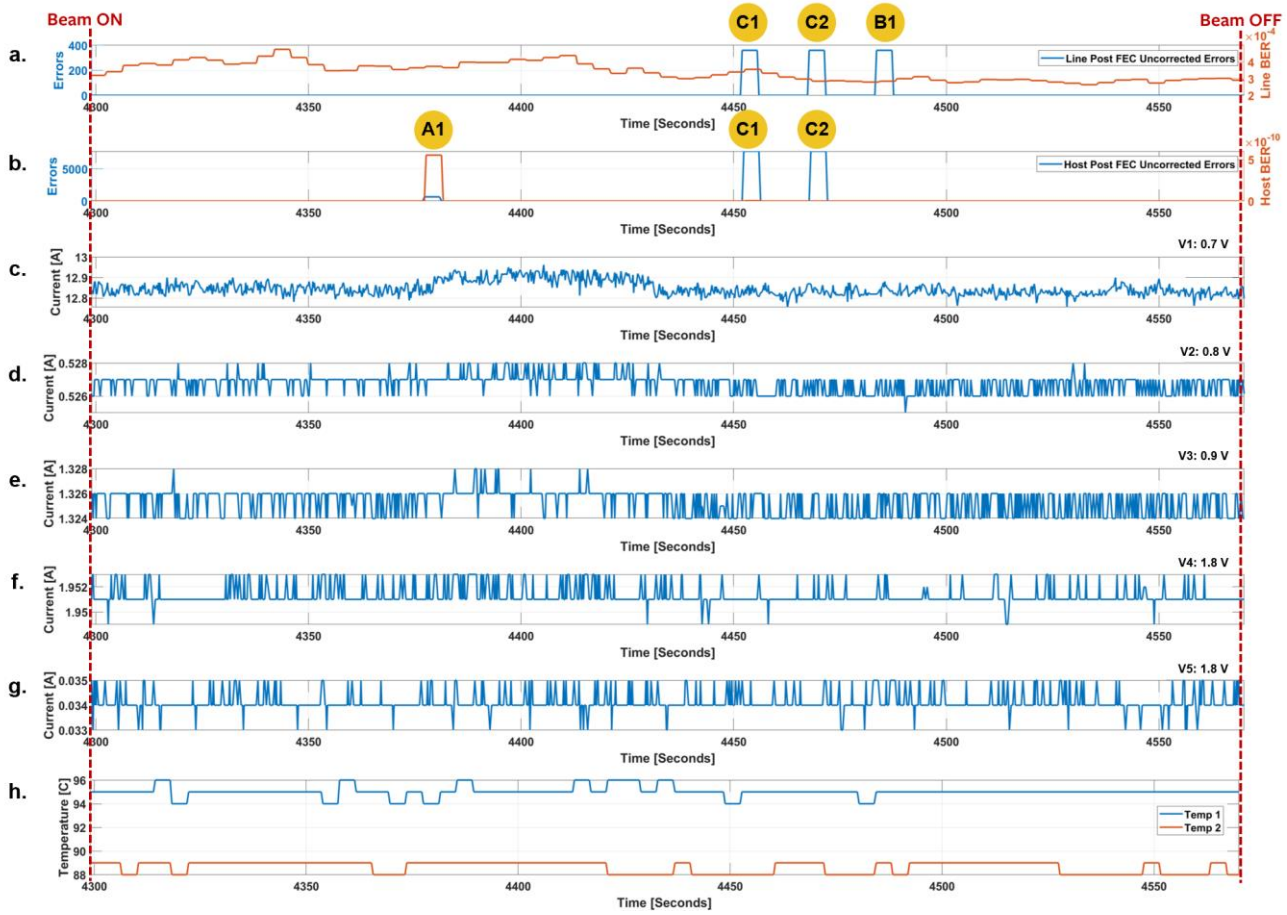

Figure 6. Data set from radiation round 2.4 with Xenon ions, showing a total of four SEUs during radiation with labels of each SEU type.

SEU type A occurred when the host post-FEC uncorrected error count was greater than zero. After a time-period of less than 8 seconds, the ASIC host FEC was able to correct all host-side errors and establish a host post-FEC uncorrected error count of zero. We observed a total of 43 occurrences of SEU type A. We observed a host post-FEC uncorrected error count ranging from 7 to 1.98×10^4, and the host post-FEC uncorrected error count remained constant during each SEU. The typical duration of this SEU was 3.6 seconds (exactly 15 timestamps from recorded data file) for 39 of the 42 total occurrences. There were 3 occurrences with a time duration of ~7.5 seconds (exactly 30 timestamps from recorded data file). We generally observed that the host post-FEC uncorrected error count during the SEU would increase with increasing LET level. Figure 6(b) shows one SEU type A with 3.6 second duration observed during radiation round 2.4 with Xenon ions, labelled A1. There were some occurrences with "stepped increase" of voltage rails V3 and V4 of in the range of tens of milliamps, but this current increase is not out of nominal range for the voltage rails.

SEU type B occurred when the line post-FEC uncorrected error count was greater than zero. We observed a line post-FEC uncorrected error count ranging from 16 to 1.49×10^3, and the line post-FEC uncorrected error count remained constant during each SEU. After a time-period of ~3.6 seconds (exactly 15 timestamps from recorded data file), the ASIC line FEC was able to correct all line-side errors and establish line post-FEC uncorrected error count of zero. We observed a total of 26 occurrences of SEU type B. We only observed type B SEUs for radiation round 2 with Xenon ions. Figure 6(a) shows one SEU type B with 3.6 second duration observed during radiation round 2.4 with Xenon ions, labelled B1.

SEU type C occurred when the line post-FEC uncorrected error count was greater than zero, and in the following time stamp the host post-FEC uncorrected error count was greater than zero. After a time-period of ~3.6 seconds, the line post-FEC uncorrected error returned to zero, and in the following time stamp the host post-FEC uncorrected error count returned to zero. Table 3 shows the data log from radiation round 2.4 with Xenon ions as an example of SEU type C. The line post-FEC uncorrected error count ranged from 350 to 552 and the host post-FEC uncorrected error count ranged from 80 to 2.95×10^4. Figure 6(a) and Figure 6(b) shows two SEU type Cs with 3.6 second duration observed during radiation round 2.4 with Xenon ions, labelled C1 and C2. We observed a total of 13 occurrences of SEU type C. There were two variations we observed of SEU type C. There was one occurrence in which the host post-FEC uncorrected error count did not return to zero in the following time stamp from the line post-FEC uncorrected error count. In this occurrence, the host post FEC uncorrected error count did not return to zero until ~ 3.6 seconds later (15 timestamps). There were two occurrences in which the host post-FEC uncorrected error count was greater than zero for a ~3.6 second time period (similar to SEU type A), followed by the line post-FEC uncorrected error count changing to a value greater than zero. In the following timestamp, the host post-FEC uncorrected error count was greater than zero. Both the line and host post-FEC uncorrected error counts returned to zero after ~3.6 seconds and in subsequent time stamps. An example of this variation of SEU type C is shown in Figure 8 from radiation round 7.2 with Xenon ions and 19 mm polyethylene degrader.

Table 3. Data log from radiation round 2.4 with Xenon ions, showing SEU type C.

Time Stamp	**Line Post-FEC Errors**	**Line Pre-FEC BER**	**Host Post-FEC Errors**	**Host Pre-FEC BER**	**Temp [C]**	**Current [Amps]**				
						V1 0.7V	**V2 0.8V**	**V3 0.9V**	**V4 0.7V**	**V5 1.8V**
4451.580	0.00E+00	3.40E-04	0.00E+00	0.00E+00	95	12.806	0.526	1.326	1.951	0.034
4451.986	**3.60E+02**	2.98E-04	0.00E+00	0.00E+00	95	12.869	0.526	1.324	1.951	0.034
4452.361	3.60E+02	2.98E-04	**7.70E+03**	0.00E+00	95	12.869	0.527	1.324	1.951	0.034
4452.768	3.60E+02	2.85E-04	7.70E+03	0.00E+00	95	12.831	0.526	1.326	1.951	0.034
4452.955	3.60E+02	2.85E-04	7.70E+03	0.00E+00	95	12.825	0.527	1.324	1.951	0.034
4453.127	3.60E+02	2.85E-04	7.70E+03	0.00E+00	95	12.85	0.526	1.326	1.953	0.034
4453.299	3.60E+02	2.85E-04	7.70E+03	0.00E+00	95	12.85	0.526	1.326	1.951	0.034
4453.471	3.60E+02	2.85E-04	7.70E+03	0.00E+00	95	12.85	0.527	1.326	1.951	0.034
4453.658	3.60E+02	2.85E-04	7.70E+03	0.00E+00	95	12.837	0.527	1.326	1.951	0.034
4453.83	3.60E+02	2.85E-04	7.70E+03	0.00E+00	95	12.844	0.527	1.326	1.951	0.034
4454.002	3.60E+02	2.85E-04	7.70E+03	0.00E+00	95	12.825	0.526	1.326	1.951	0.034

4454.19	3.60E+02	2.85E-04	7.70E+03	0.00E+00	95	12.825	0.527	1.326	1.953	0.034
4454.361	3.60E+02	2.85E-04	7.70E+03	0.00E+00	95	12.819	0.527	1.324	1.951	0.034
4454.768	3.60E+02	2.85E-04	7.70E+03	0.00E+00	95	12.825	0.527	1.324	1.951	0.034
4455.143	3.60E+02	2.85E-04	7.70E+03	0.00E+00	95	12.863	0.526	1.324	1.951	0.034
4455.533	**3.60E+02**	2.85E-04	7.70E+03	0.00E+00	95	12.812	0.527	1.324	1.951	0.035
4455.924	0.00E+00	2.85E-04	**7.70E+03**	0.00E+00	95	12.837	0.526	1.324	1.951	0.035
4456.315	0.00E+00	2.85E-04	0.00E+00	0.00E+00	95	12.831	0.526	1.326	1.951	0.034

3.2 Observed Heavy Ion Single Event Functional Interrupts

We define a single event functional interrupt (SEFI) as an anomalous event that required a soft reset or hard reset of the OMA to re-establish nominal functionality. The anomalous behavior and GUI error messages did not disappear or self-correct after a period of more than 12 seconds. There were three types of SEFIs observed during radiation testing.

SEFI type A occurred when both the line and host pre-FEC BER changed to values of "-1," indicating an erroneous state of the DUT. GUI error messages of the line side lost lock continuously appeared during the SEFI, even after the radiation round was completed and the DUT was no longer exposed to heavy ions. Two occurrences of SEFI type A were observed, once in radiation round 2.5 and once in radiation round 2.6 with Xenon ions. In radiation round 2.5, the line side and host side post-FEC uncorrected error counts were zero prior to the SEFI occurring, and the line-side pre-FEC BER was 2.67×10^{-4}. The line and host pre-FEC BER changed to "-1" at the same timestamp. We completed a soft reset prior to radiation round 2.6, restoring nominal line and host side pre-FEC BERs and the error message no longer appeared. Figure 7 shows the data graph from radiation round 2.5 with the SEFI indicated with label "A". Near the end of radiation round 2.6, we observed the second occurrence of SEFI type A. The line side pre-FEC BER was 2.38×10^{-4} prior to the SEFI, and a SEU type C had resolved one time stamp before the SEFI occurrence. The line side pre-FEC BER changed to the "-1" error state four seconds prior to the host side pre-FEC BER changed to "-1" error state. The error message and BER state of "-1" continued even after the heavy ion beam was off. We observed the SEFI for two minutes after the beam was off, then performed a soft reset. The soft reset restored nominal functionality.

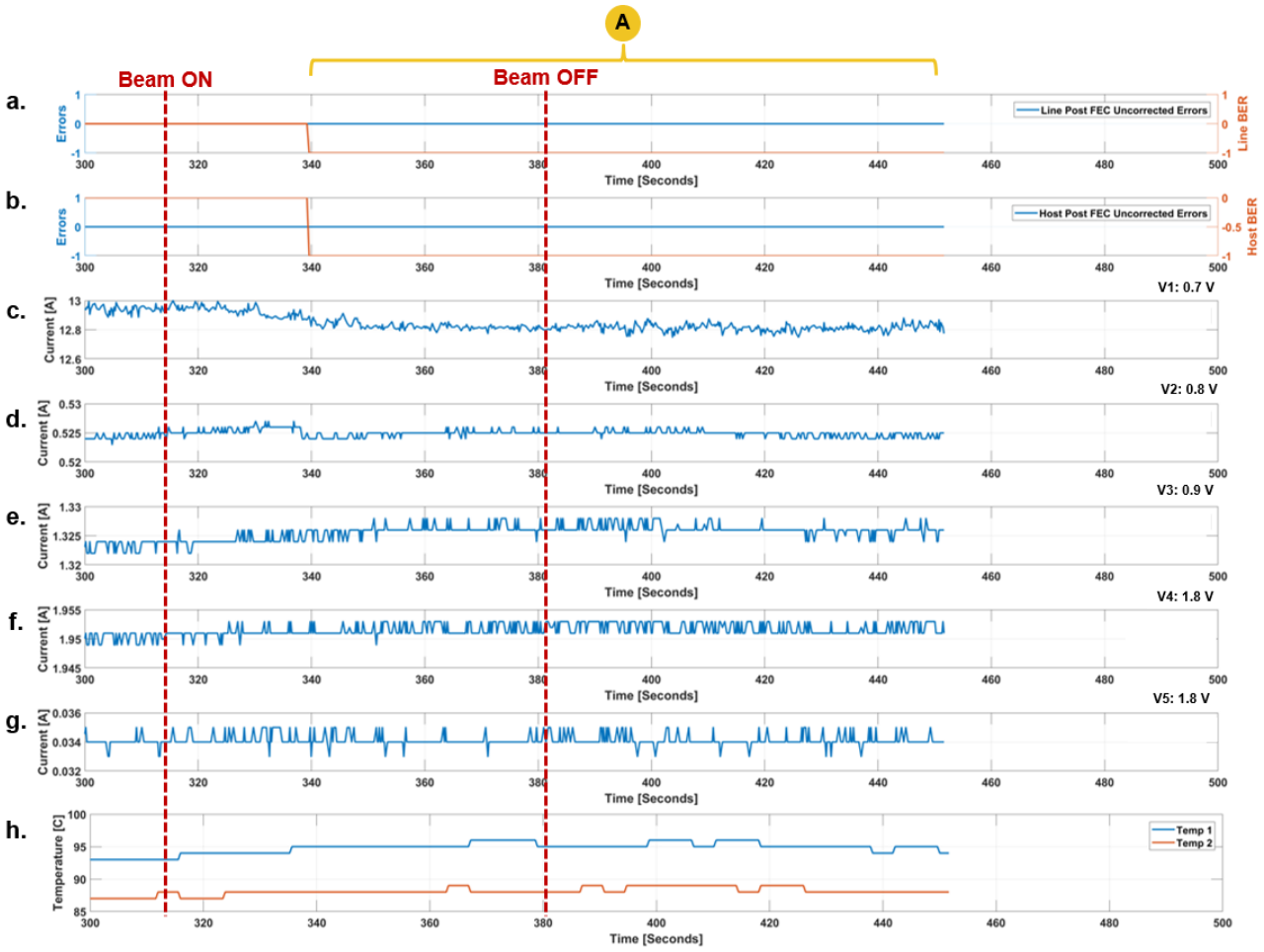

Figure 7. Data graphs from radiation round 2.5 with Xenon ions. SEFI type A with line side and host side pre-FEC BER in error state of "-1" and error state continued even after heavy ion beam was off.

SEFI type B occurred when the host side post-FEC error count was greater than zero for a time period of over 12 seconds and an error message for the host post FEC errors appeared continuously on the GUI. The host side post-FEC non-zero error count and error message continued even after the heavy ion beam was off and hard reset was required to establish nominal functionality. We observed three occurrences of SEFI type B. We observed a SEFI type B in radiation round 2.7 with xenon ions. The host side post-FEC error count was 4.09×10^7 when the SEFI began. Prior to the SEFI (3.4 seconds), we observed a stepped decrease in current of the analog voltage rails V3 and V4, but the change in current is not significant. Voltage rail V3 decreased by 20 mA and V4 decreased by ~100 mA. We performed two soft resets of the OMA, both of which were not successful in restoring nominal functionality and the host side post-FEC error message continued to appear on the GUI after each soft reset. A hard reset successfully re-established nominal functionality.

The second observation of SEFI type B occurred during radiation round 5 with xenon ions and 17 mm of polyethylene degrader. The third SEFI type B occurred during radiation round 7.2 with Xenon ions and 19 mm of polyethylene degrader. The host side post-FEC error count was 9280 during the SEFI, and we observed a slight stepped current increase in the analog power supply voltage rails. Voltage rail V3 increased by 12 mA and V4 increased by 50 mA. The increased current levels are within nominal range of the voltage rails. Figure 8 shows the data graphs from radiation round 7.2 with Xenon ions and 19 mm of polyethylene degrader. SEFI type B and the stepped current increase in voltage rails V3 and V4 are labelled.

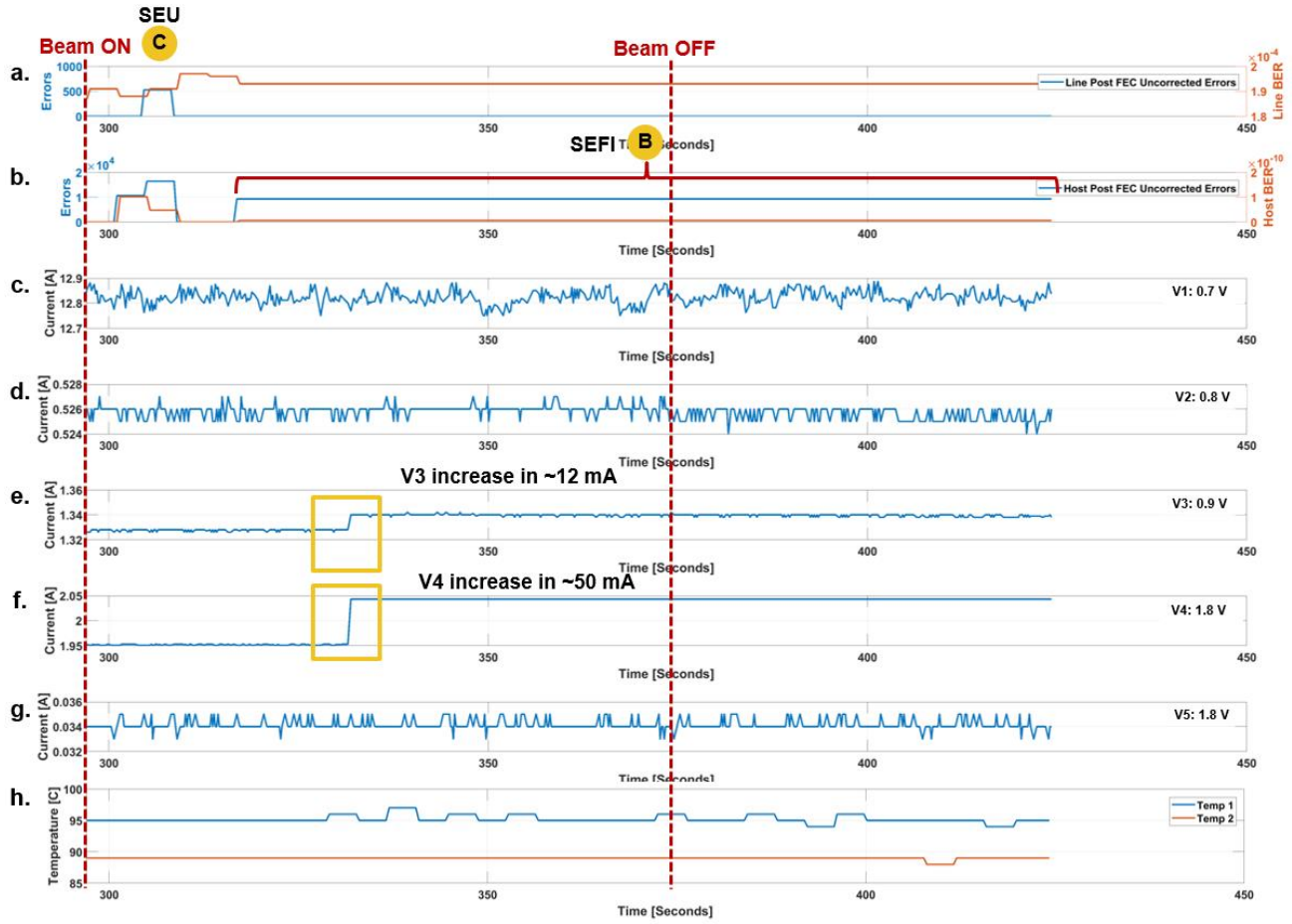

Figure 8. Data graphs from radiation round 7.2 with Xenon ions and 19 mm of polyethylene degrader. SEFI type B, SEU type C, and the stepped current increase in voltage rails V3 and V4 are labelled.

SEFI type C occurred when a GUI error message associated with the SPI data polling appeared and data recording was stopped. We observed the error message would repeat on the GUI and no data was logged in the telemetry file. After a 70 second period, there was nominal functionality and data was logged. The error behavior repeated later during the radiation round, even when the heavy ion beam was off. A hard reset was required to establish nominal functionality and prevent the error from re-appearing in a subsequent radiation round. The first occurrence of SEFI type C was in radiation rounds 2.8 and 2.9 with Xenon ions. The first set of error messages appeared after the beam was off in radiation round 2.8. We did not perform any reset after radiation round 2.8 since the error message disappeared and nominal functionality was established after ~70.3 seconds. During radiation round 2.9, the type C anomalous behavior (missing data logging over ~ 70.3 second periods) repeated three times during irradiation and two times after the beam was off. We performed a hard reset after radiation round 2.9 and did not observe SEFI type C in radiation round 3. The second occurrence of SEFI type C was in radiation round 4 with Xenon ions and 16 mm of polyethylene degrader. The first error messages and missing data logging over ~26.3 second period occurred ~4.8 seconds after the beginning of the radiation round. There were three instances after the beam was off with similar anomalous behavior with missing data logging over ~26.3, ~30.7, and ~25.6 second periods. A hard reset was performed after radiation round 4. Figure 9 shows the data graphs from radiation round 4 with Xenon ions and indicates the missing recorded data. The third occurrence of SEFI type C was in radiation round 7.1 with Xenon ions and 19 mm of polyethylene degrader. Immediately when the beam was turned on, we observed the SPI data polling error repeat on the GUI and no data was recorded in the telemetry file. A hard reset was performed and we did not observed the SEFI type C behavior in radiation round 7.2.

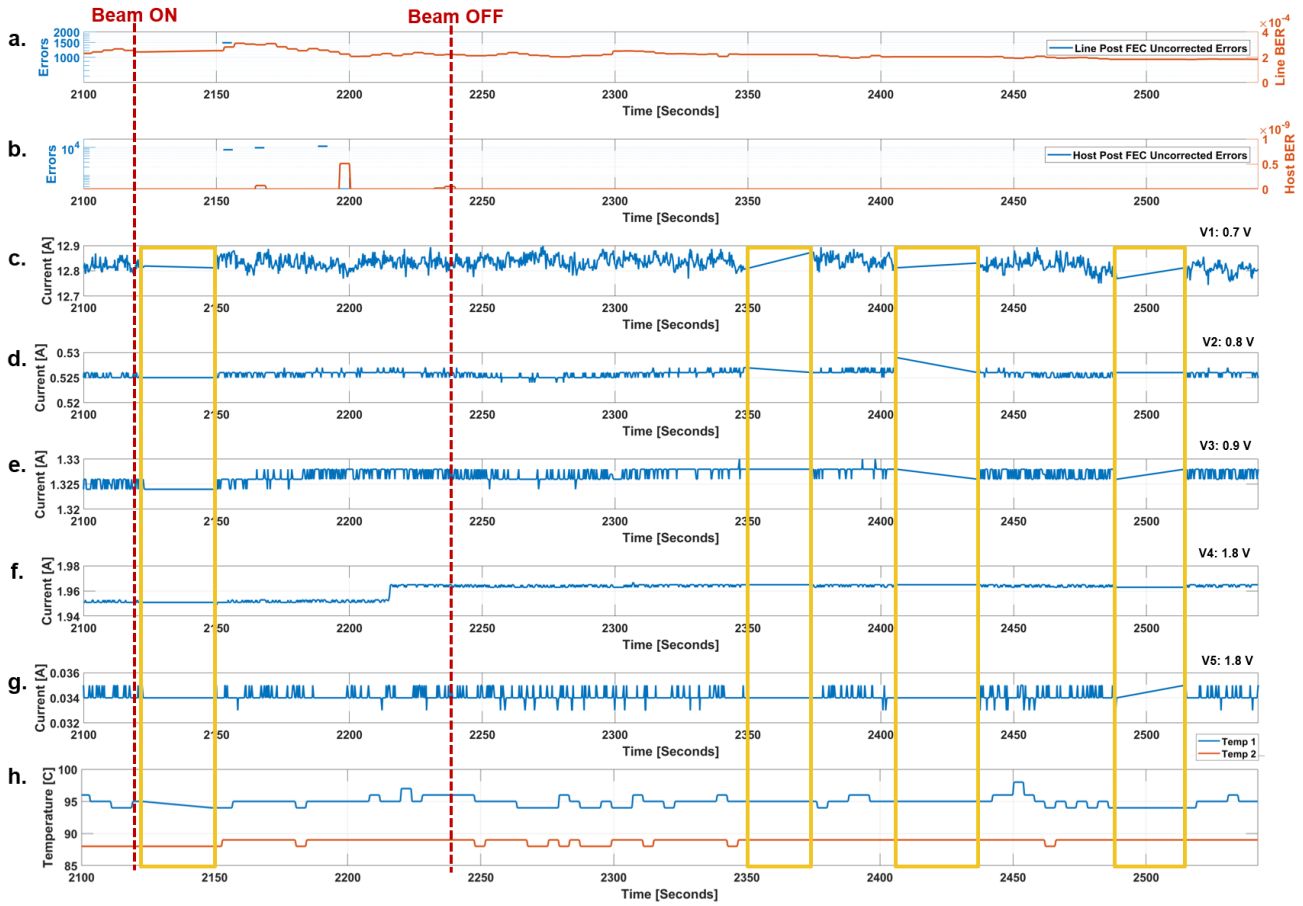

Figure 9. Data graphs from radiation round 4 with Xenon ions and 16 mm polyethylene degrader to show SEFI type C behavior with missing data logging.

4. CONCLUSIONS

We performed heavy ion radiation testing on a commercial optical coherent DSP ASIC with 16 nm FinFET plus CMOS technology. No destructive heavy ion SEEs were observed. We observed three types of SEUs, which were based on the line side and host side post-FEC uncorrected error count, and nominal functionality was typically re-established in ~3.6 seconds. We observed three types of SEFIs, which were based on the line side and host side BER in an error state, extended duration of non-zero host side post-FEC uncorrected error count, and a SPI data polling error. A reset was required to restore nominal function of the ASIC after a SEFI was observed.

This work was focused on characterizing heavy ion induced SEEs on the commercial optical coherent DSP ASIC and screening for destructive heavy ion SEEs. Future work will include additional heavy ion and proton test campaigns of the device to further characterize SEEs and gather more data at different energy levels. We will calculate the associated LET levels from the radiation rounds of this heavy ion test campaign as well as the future test campaigns. The LET levels and the heavy ion SEE cross section data from this test campaign and future test campaigns will be used to determine heavy ion SEE rates for various space missions.

REFERENCES

[1] Robinson, Boroson, Schieler, Khatri, Guldner, Constantine, Shih, Burnside, Bilyeu, Hakimi, Garg, Allen, Clements, Cornwell, "TeraByte InfraRed Delivery (TBIRD): a demonstration of large-volume direct-to-Earth data transfer

from low-Earth orbit ," Proc. SPIE 10524, Free-Space Laser Communication and Atmospheric Propagation XXX, 105240V (15 February 2018); doi: 10.1117/12.2295023

[2] LaBel, Kenneth A., et al. "On the suitability of fiber optic data links in the space radiation environment: a historical and scaling technology perspective." Aerospace Conference, 1998 IEEE. Vol. 4. IEEE, 1998.

[3] Aniceto, Raichelle J., et al. "Single Event Effect and Total Ionizing Dose Assessment of Commercial Optical Coherent DSP ASIC." Nuclear and Space Radiations Effects Conference (NSREC) (2017), Data Workshop.

[4] Aniceto, Raichelle J., et al. “Assessment of Gamma and Proton Radiation Effects on 100 Gbps Commercial Coherent Optical Transceiver.” International Conference on Space Optics (ICSO) (2018), Data Workshop.

[5] Karp, James, et al. "Single-Event Latch-Up: Increased Sensitivity From Planar to FinFET." IEEE Transactions on Nuclear Science 65.1 (2018): 217-222.